Combined vacuum ultraviolet laser and synchrotron pulsed field ionization study of CH_2BrCl

Cite as: J. Chem. Phys. **126**, 184304 (2007); https://doi.org/10.1063/1.2730829
Submitted: 14 March 2007 • Accepted: 23 March 2007 • Published Online: 11 May 2007

Juan Li, Jie Yang, Yuxiang Mo, et al.

Combined vacuum ultraviolet laser and synchrotron pulsed field ionization study of CH_2BrCl

Juan Li, Jie Yang, and Yuxiang Mo[a)]
Key Laboratory for Atomic and Molecular Nanosciences, Department of Physics, Tsinghua University, Beijing 10084, China

K. C. Lau[b)]
Department of Biology and Chemistry, City University of Hong Kong, Kowloon, Hong Kong

X. M. Qian, Y. Song, Jianbo Liu, and C. Y. Ng[c)]
Department of Chemistry, University of California, Davis, Davis, California 95616

(Received 14 March 2007; accepted 23 March 2007; published online 11 May 2007)

The pulsed field ionization-photoelectron (PFI-PE) spectrum of bromochloromethane (CH_2BrCl) in the region of 85 320–88 200 cm^{-1} has been measured using vacuum ultraviolet laser. The vibrational structure resolved in the PFI-PE spectrum was assigned based on *ab initio* quantum chemical calculations and Franck-Condon factor predictions. At energies 0–1400 cm^{-1} above the adiabatic ionization energy (IE) of CH_2BrCl, the Br–C–Cl bending vibration progression ($\nu_1^+=0-8$) of CH_2BrCl^+ is well resolved and constitutes the major structure in the PFI-PE spectrum, whereas the spectrum at energies 1400–2600 cm^{-1} above the IE(CH_2BrCl) is found to exhibit complex vibrational features, suggesting perturbation by the low lying excited $CH_2BrCl^+(\tilde{A}\,^2A'')$ state. The assignment of the PFI-PE vibrational bands gives the IE(CH_2BrCl) $=85\,612.4\pm2.0$ cm^{-1} (10.6146±0.0003 eV) and the bending frequencies $\nu_1^+(a_1')=209.7\pm2.0$ cm^{-1} for $CH_2BrCl^+(\tilde{X}\,^2A')$. We have also examined the dissociative photoionization process, $CH_2BrCl+h\nu\rightarrow CH_2Cl^++Br+e^-$, in the energy range of 11.36–11.57 eV using the synchrotron based PFI-PE-photoion coincidence method, yielding the 0 K threshold or appearance energy AE(CH_2Cl^+)=11.509±0.002 eV. Combining the 0 K AE(CH_2Cl^+) and IE(CH_2BrCl) values obtained in this study, together with the known IE(CH_2Cl), we have determined the 0 K bond dissociation energies (D_0) for CH_2Cl^+-Br (0.894±0.002 eV) and CH_2Cl-Br (2.76±0.01 eV). We have also performed CCSD(T, full)/complete basis set (CBS) calculations with high-level corrections for the predictions of the IE(CH_2BrCl), AE(CH_2Cl^+), IE(CH_2Cl), $D_0(CH_2Cl^+-Br)$, and $D_0(CH_2Cl-Br)$. The comparison between the theoretical predictions and experimental determinations indicates that the CCSD(T, full)/CBS calculations with high-level corrections are highly reliable with estimated error limits of <17 meV. © *2007 American Institute of Physics*. [DOI: 10.1063/1.2730829]

I. INTRODUCTION

Halogenated hydrocarbons have been widely used in many industrial and domestic applications. The release of these compounds into the atmosphere has lead to serious environmental problems.[1–4] Since halogen-containing hydrocarbons are resistant to chemical decomposition and biodegradation, they have long atmospheric lifetimes at low atmospheric altitudes.[4] At high altitudes, solar UV radiation is effective in breaking down halogen-containing molecules, such as CH_2BrCl, by photodissociation to release the halogen atoms. Halogen atoms thus formed are believed to be responsible for the catalytic decomposition of the ozone layer of the Earth's stratosphere.[1,2] For this reason, many previous UV excimer laser photodissociation studies of halogenated hydrocarbons in the laboratory[5,6] were aimed to understand the production of halogen atoms from these compounds.

The modeling of the chemistry of halogenated hydrocarbons in the atmosphere also requires reliable thermochemical properties, such as 0 K bond dissociation energies (D_0), of the halogen-containing hydrocarbons. Vacuum ultraviolet (VUV) photoionization mass spectrometry and photoelectron spectroscopy are well established techniques for thermochemical measurements of neutral and ionic species.[7] The recent development of the synchrotron based pulsed field ionization photoelectron-photoion coincidence (PFI-PEPICO) time-of-flight (TOF) technique[8,9] has allowed the unambiguous determination of the 0 K dissociative photoionization thresholds or appearance energies (AEs) for simple molecular species, achieving a precision limited only by the PFI-PE measurements.[7–16] Using the 0 K AE thus determined, together with the adiabatic ionization energy (IE) measurements by the VUV laser PFI-PE method, we

[a)]Electronic mail: ymo@mail.tsinghua.edu.cn
[b)]Electronic mail: kaichung@cityu.edu.hk
[c)]Electronic mail: cyng@chem.ucdavis.edu

have previously determined highly precise D_0 values for many simple molecules and their ions.[7,17] The 0 K heats of formation (ΔH_{f0}) of the fragments and parent and their ions are related by the thermochemical cycles. Thus, precise IE and 0 K AE values obtained by PFI measurements can also be used to determine precise ΔH_{f0} values for the neutral fragments and parent and their ions.[11–14]

This report presents the result of a combined VUV laser PFI-PE and synchrotron PFI-PEPICO study of CH_2BrCl. Due to the small Franck-Condon factor (FCF) expected for the 0-0 photoionization transition resulting from a big geometry difference between the neutral and the cation, the accurate determination of the adiabatic IE of CH_2BrCl by photoionization efficiency (PIE) and/or photoelectron measurement can be difficult. The previous PIE[18] and He I photoelectron[19] measurements gave an IE(CH_2BrCl) value of 10.77±0.01 eV. As shown below, the assignment of the VUV laser PFI-PE spectrum of CH_2BrCl yields a significantly lower IE(CH_2BrCl) value compared to the previous PIE and He I value. The IE(CH_2BrCl) and AE for the formation of CH_2Cl^+ [AE(CH_2Cl^+)] from CH_2BrCl determined here represent the current most precise experimental measurements. Combining the IE(CH_2BrCl) and AE(CH_2Cl^+) values determined by PFI measurements along with the known IE(CH_2Cl) reported in the previous He I photoelectron study, we have obtained more precise values for the $D_0(CH_2Cl-Br)$ and $D_0(CH_2Cl^+-Br)$. The AE(CH_2Cl^+) =11.6±0.1 eV was measured first by Harrison and Shannon in an electron impact study.[20] Following our PFI-PEPICO measurement,[17,21] Lago *et al.*[22] have reexamined the AE(CH_2Cl^+) value using a variant of the threshold photoelectron-photoion coincidence technique using electron imaging optics. Their result is found to be in excellent agreement with the PFI-PEPICO value.

For guiding the assignment and interpretation of the PFI-PE spectrum of CH_2BrCl, we have carried out theoretical *ab initio* quantum calculations for the harmonic and anharmonic vibrational frequencies of CH_2BrCl and CH_2BrCl^+ and FCFs associated with the $CH_2BrCl^+(\tilde{X}) \leftarrow CH_2BrCl(\tilde{X})$ photoionization transitions. The precise experimental values for the IE(CH_2BrCl), AE(CH_2Cl^+), $D_0(CH_2Cl-Br)$, and $D_0(CH_2Cl^+-Br)$ obtained in this study can be used to benchmark state-of-the-art theoretical predictions. Thus, we have undertaken high-level *ab initio* quantum calculations on the IE, AE, and D_0 values for the CH_2BrCl^+/CH_2BrCl and CH_2Cl^+/CH_2Cl system at the coupled cluster level with single and double excitations pluse quasiperturbative triple excitations [CCSD(T, full)] along with approximations to the complete basis set (CBS) limits.[17,23–25] Furthermore, high-level corrections were also made in these calculations.[17]

II. EXPERIMENT

A. VUV laser PFI-PE measurements

The VUV photoelectron and photoion spectrometer used in this experiment has been described previously.[26,27] Briefly, coherent VUV radiation was generated by using the resonance enhanced four-wave difference-frequency mixing in a pulsed Kr jet. The fundamental frequencies were generated by two dye lasers, which were pumped by the same Nd-yttrium aluminum garnet (YAG) laser (20 Hz). One dye laser frequency (ω_1) was fixed to match the two-photon ($2\omega_1$) resonance frequency of the Kr, $4p^5(^2P_{1/2})5p[1/2]_0 \leftarrow (4p^6)^1S_0$ transition at 98 855.1 cm^{-1}. The frequency (ω_2) of the other dye laser beam was tuned from 940 to 730 nm. The laser output range of 940–800 nm was obtained by Raman shifting of the dye laser output from 676 to 600 nm in a H_2 Raman cell. The two fundamental laser beams with frequencies ω_1 and ω_2 were merged by a dichroic mirror and focused by an achromatic lens onto a pulsed Kr jet. The VUV laser radiation of interest is selected by the VUV monochromator before intersecting perpendicularly with the molecular sample beam at the photoionization region.

The apparatus consists of four vacuum chambers: namely, the beam source chamber, which houses a pulsed valve (nozzle diameter=0.7 mm) to produce a pulsed molecular beam of the CH_2BrCl gas sample, the frequency-mixing chamber, which houses the pulsed Kr jet (nozzle diameter=1 mm), the monochromator chamber, which is equipped with a gold coated toroidal grating, and the ionization chamber, which houses ion and electron TOF spectrometers together with a set of dual microchannel plate (MCP) detectors for charged particle detection. The pulsed CH_2BrCl beam produced in the beam source chamber is skimmed by circular skimmer (diameter=1 mm) before entering the photoionization chamber. The lengths of the drift regions for the ion and electron TOF spectrometers are 80 and 26 cm, respectively. Two layers of μ-metal shield are installed inside the ionization chamber. A separate MCP detector is used in this chamber to monitor the VUV laser intensity.

The electron and VUV radiation signals from the MCP detectors were fed into two identical boxcars (SR 245, Stanford Research Systems) and transferred to a personal computer. The pulses to synchronize the two pulsed valves and the Nd-YAG laser were provided by a digital delay generator (DG 535, Stanford Research Systems). The PFI voltage pulses (≈1.5 V/cm) for Stark ionization of high-n Rydberg molecules were provided by another DG 535 unit. The delay between the VUV excitation laser and the PFI voltage pulse was typically 3 μs. The effects of the applied electric field in decreasing the ionization energies have been corrected for the PFI-PE spectra presented here.

The vapor pressure of pure CH_2BrCl (purity=99%, Sigma-Aldrich) at room temperature was used as the stagnation pressure to produce the skimmed pulsed supersonic beam (20 Hz). During the experiments, the pressures for the beam source and ionization chambers were maintained at $\approx 1.5\times10^{-5}$ and 1.5×10^{-7} Torr, respectively. To avoid sampling of CH_2BrCl dimers and clusters, we find that it is necessary to time the VUV laser to hit the early part of the molecular beam pulse. The frequencies of the dye lasers were calibrated by He/Ne and He/Ar optogalvanic lamps.

B. VUV synchrotron PFI-PEPICO TOF measurements

The PFI-PEPICO TOF measurements for CH_2BrCl were conducted using the high-resolution VUV photoelectron-photoion facility of the Chemical Dynamics Beamline at the

Advanced Light Source (ALS).[28–30] The procedures for PFI-PEPICO TOF measurements have been described in detail previously.[8–16] The experiment was performed at the multibunch mode (period=656 ns, dark gap=104 ns). In this experiment, Ar was used in the gas filter to suppress higher undulator harmonics with photon energies greater than 15.759 eV. A 2400 lines/mm grating (dispersion =0.64 Å/mm) was used to disperse the first order harmonic of the undulator VUV beam with entrance/exit slits set in the range of 30–100 μm. The resulting monochromatic VUV beam was then focused into the photoionization region of the photoelectron-photoion apparatus.

The application of the PFI pulse (height=9 V/cm, width=200 ns) was delayed by 10 ns with respect to the beginning of the dark gap. The PFI pulse also served to extract photoions towards the ion detector. The average accumulation time for a PFI-PEPICO TOF spectrum at a fixed VUV energy was about 30 min. The photon energy ($h\nu$) calibration was achieved using the $Ar^+(^2P_{3/2})$, $Xe^+(^2P_{3/2})$, and $NO^+(X\ ^1\Sigma^+, v^+=0)$ PFI-PE bands[28,30,31] recorded under the same experimental conditions before and after each scan. The Stark shift correction of the energy scale for the PFI-PEPICO measurement of CH_2BrCl was made based on the assumption that the Stark shifts of the present PFI-PEPICO measurements are identical to those observed for the rare gases and NO measured under the same experimental conditions.

The CH_2BrCl gas sample (purity=99.9%, Aldrich) at room temperature was introduced into the photoionization region as a pure, continuous skimmed supersonic beam (nozzle diameter=127 μm) as described previously.[8–16] The photoionization chamber was maintained at a pressure of $<10^{-6}$ Torr during the experiment.

III. THEORETICAL CONSIDERATIONS

A. High-level *ab initio* quantum calculations

The $IE[CH_2ClBr(\tilde{X}\ ^1A') \rightarrow CH_2ClBr^+(\tilde{X}\ ^2A')]$ and $AE(CH_2ClBr \rightarrow CH_2Cl^+ + Br)$ were calculated with the fully *ab initio* wave function based CCSD(T, full)/CBS extrapolation procedures, which involve the approximation to the CBS limit at the CCSD(T) level.[32] These procedures used here explicitly incorporate the zero-point vibration energy (ZPVE) correction, the core-valence (CV) electronic correlation correction, the scalar-relativistic (SR) correction, and the spin-orbit (SO) coupling. The CCSD(T, full)/CBS procedure with these high-level corrections,[17,23–25] which will be referred to as CCSD(T)/CBS procedure below, was originally used by Dixon *et al.*,[33] and is currently a state-of-the-art theoretical method for thermochemical predictions.

The CCSD(T)/CBS procedure for IE and AE calculations has been described previously in detail.[17,23–25] In the present calculations, the geometry optimizations for CH_2Cl and CH_2BrCl and their cations were calculated at the CCSD(T)/6-311++G(2df,p) level of theory. We have listed in Table I the bond lengths (r) in angstrom and bond angles ($\angle$) in degree obtained for CH_2BrCl and CH_2BrCl^+ at CCSD(T)/6-311++G(2df,p) level of theory. Based on the optimized geometries, single point energy calculations were carried out at the CCSD(T)/aug-cc-pV(X+d)Z/aug-cc-pVXZ level,[34] in which the aug-cc-pV(X+d)Z basis was used on Cl atom and regular aug-cc-pVXZ basis sets were used on other atoms. Only the valence electrons (i.e., 1s on H, 2s/2p on C, 3s/3p on Cl, and 4s/4p on Br) are correlated in the calculations. The valence CBS energies ($E_{\text{extrapolated CBS}}$) were estimated by the following two different extrapolation schemes:

TABLE I. Comparison of bond lengths (r) in angstrom and bond angles ($\angle$) in degree obtained for CH_2BrCl and CH_2BrCl^+ at CCSD(T)/6-311++G(2df,p) level of theory.

	CH_2ClBr (C_s, $^1A'$)	CH_2ClBr^+ (C_s, $^2A'$)	Δ (ion-neutral)[a]
r(C–Cl)	1.773	1.770	–0.003
r(C–Br)	1.940	1.952	0.012
r(C–H)	1.087	1.088	0.001
∠ (Br–C–Cl)	113.0	91.5	–21.5
∠ (H–C–H)	111.8	117.0	5.2
∠ (Br–C–H)	107.5	110.5	3.0
∠ (Cl–C–H)	108.6	112.2	3.6

[a]Defined as the difference (ion-neutral) in bond length or bond angle.

(i) A three-point extrapolation scheme[35] using the mixed exponent/Gaussian function of the form

$$E(X) = E_{\text{extrapolated CBS}} + B\exp[-(X-1)] + C\exp[-(X-1)^2], \quad (1)$$

where X=3, 4, and 5 are for the aug-cc-pVTZ, aug-cc-pVQZ, and aug-cc-pV5Z basis sets, respectively. Here, we denote the CBS energies extrapolated directly from the CCSD(T) valence energy using Eq. (1) with successive aug-cc-pV[T-5]Z basis sets as CBS_{TQ5}.

(ii) A two-point extrapolation scheme[36] involving the reciprocal of X^3,

$$E(X) = E_{\text{extrapolated CBS}} + \frac{B}{X^3}, \quad (2)$$

where X=4 and 5 are for the aug-cc-pVQZ and aug-cc-pV5Z basis sets, respectively. We denote the extrapolated CBS energies directly from the CCSD(T) valence energy using Eq. (2) with basis sets of cc-pV[Q,5]Z as CBS_{Q5}.

To account for the ZPVE corrections (ΔE_{ZPVE}), we have computed the harmonic vibrational frequencies and anharmonicities using second-order perturbative vibrational treatment. Under this scheme, it has been shown[37] that the ZPVE can be approximated as the average between the ZPVE from harmonic frequencies ($\text{ZPVE}_{\text{harm}}$) and that from anharmonic frequencies ($\text{ZPVE}_{\text{anharm}}$), i.e.,

$$\text{ZPVE} = \tfrac{1}{2}(\text{ZPVE}_{\text{harm}} + \text{ZPVE}_{\text{anharm}}). \quad (3)$$

The zero-order vibrational term is assumed to be small and is not included in the above approximation. The $\text{ZPVE}_{\text{harm}}$ is essentially taken as the half sum $[\Sigma_{i=1}^{3N-6}(1/2)\omega_i]$, where N is the number of atoms, ω_i's are harmonic vibrational frequencies calculated at the CCSD(T) level. The $\text{ZPVE}_{\text{anharm}}$ were

TABLE II. Theoretical and experimental anharmonic (AH) vibrational frequencies (cm^{-1}) of $CH_2BrCl(\tilde{X}\,^1A')$ and $CH_2BrCl^+(\tilde{X}\,^2A')$. All theoretical calculations are made using the 6-311++G(2df,p) basis set.

	MP2		B3LYP		CCSD(T)					
					AH(MP2)		AH(B3)		Experiment	
Neutral/cation	Neutral	Cation	Neutral	Cation	Neutral	Cation	Neutral	Cation	Neutral[a]	Cation[b]
$\nu_1(a')/\nu_1^+(a')$	230 (−2)	289 (−81)	220 (8)	212 (−4)	224 (4)	216 (−6)	224 (14)	227 (−17)	228	209.7
$\nu_2(a')/\nu_2^+(a')$	630 (−28)	575	582 (19)	517	609 (−6)	531	607 (−4)	530	603	534[c]
$\nu_3(a')/\nu_3^+(a')$	759 (−31)	742	699 (−29)	707	738 (−10)	728	736 (−8)	725	728	···
$\nu_4(a'')/\nu_4^+(a'')$	861 (−11)	916	843 (7)	893	852 (−2)	897	854 (−4)	900	850	···
$\nu_5(a'')/\nu_5^+(a'')$	1151 (−21)	1047	1123 (7)	1043	1139 (−9)	1034	1140 (−10)	1037	1130	···
$\nu_6(a')/\nu_6^+(a')$	1251 (−24)	1188	1228 (1)	1184	1243 (−16)	1182	1246 (−19)	1182	1227	···
$\nu_7(a')/\nu_7^+(a')$	1433 (−26)	1420	1413 (−6)	1401	1426 (−19)	1407	1431 (−24)	1408	1407	···
$\nu_8(a')/\nu_8^+(a')$	3026 (−38)	3028	3001 (−13)	3004	3000 (−12)	3002	2998 (−10)	3003	2988	···
$\nu_9(a'')/\nu_9^+(a'')$	3091 (−31)	3127	3063 (3)	3097	3061 (−1)	3100	3058 (2)	3100	3060	···

[a]Reference 46.
[b]This work.
[c]Value obtained from the assignment of the combination band $\nu_1^+(a')+\nu_2^+(a')=744\ cm^{-1}$. See the text.

taken to be the half sum $[\Sigma_{i=1}^{3N-6}(1/2)\upsilon_i]$ of the anharmonic vibrational frequencies (υ_i) calculated effectively at the CCSD(T) level. To obtain the anharmonic (AH) vibrational frequencies, we first calculated the harmonic (H) vibrational frequencies at the CCSD(T) level, together with the harmonic frequencies and anharmonic effects at the MP2 and B3LYP levels. The CCSD(T) harmonic vibrational frequencies are then corrected with the anharmonicities obtained at the MP2 and the hybrid B3LYP exchange-correlation functional levels to yield the respective anharmonic vibrational frequencies AH(MP2) and AH(B3) effectively at the CCSD(T) level of theory. Both the anharmonic and harmonic vibrational frequencies calculations were done using the 6-311++G(2df,p) basis set. Table II summaries the H and AH vibrational frequencies calculated at the MP2/6-311++G(2df,p), B3LYP/6-311++G(2df,p), and CCSD(T)/6-311++G(2df,p) levels of theory.

The CV energy (E_{CV}) takes into account the electronic correlation contributions between the core and valence electrons and those within the core electrons. The aug-cc-pwCVQZ basis set[38] is used to recover CV electronic correlations during the ionization and dissociative ionization processes. The E_{CV} is defined in the following way:

$$E_{CV} = E[\text{CCSD(T,core + valence)/aug-cc-pwCVQZ}] - E[\text{CCSD(T,valence)/aug-cc-pwCVQZ}], \quad (4)$$

where the E[CCSD(T,valence)] is the energy with only valence electrons correlated and the E[CCSD(T,core+valence)] is the energy with both core and valence electrons correlated at the CCSD(T) level of theory. The core electrons to be correlated are the $1s$ electrons on carbon atom, $2s/2p$ electrons on chlorine atom, and $3s/3p/3d$ electrons on bromine atom.

The SR energy (E_{SR}) is computed using the configuration interaction with the singles and doubles (CISD) theory and the aug-cc-pV5Z basis set based on the corresponding optimized geometries. The E_{SR} is taken as the sum of the mass-velocity and one-electron Darwin terms in the Breit-Pauli Hamiltonian.[39] The atomic spin-orbit correction (E_{SO}) of −0.152 eV for Br is based on the experimental excitation energies of Moore.[40] The molecular spin-orbit coupling in the $CH_2ClBr^+(^2A')$ was computed by first order perturbation theory. The calculations used an uncontracted cc-pVTZ basis set [only the (s,p) functions on H, the (s,p,d) functions on C and Cl, and the (s,p,d,f) functions on Br were used]. Spin-orbit matrix elements were computed among the components of the $CH_2ClBr^+(^2A')$ and $CH_2ClBr^+(^2A'')$ states using the internally contracted multireference configuration interaction wave function.[41] The $1s$ electrons on carbon and chlorine as well as the $1s/2s/2p$ electrons on Br were not included in the active space.

All CCSD(T) single-point energy calculations, vibrational frequency calculations, and correlation contributions were performed using the MOLPRO 2002.6 program suite.[42] The harmonic and anharmonic vibrational frequencies at MP2 and B3LYP levels were calculated using the GAUSSIAN-03 program package.[43]

B. Franck-Condon factor calculations

The FCF simulations of the PFI-PE spectrum were carried out with the MOMOFCF program from Iwata's group.[44,45] The simulations assume the potential energy surfaces of both CH_2BrCl and CH_2BrCl^+ are harmonic and take into account the Duschinsky effect. The CCSD(T)/6-311++G(2df,p) optimized geometries, vibrational frequencies, and normal mode displacement vectors are used. Due to the weak intensities in the higher order overtones, we have limited the number of transitions involved in the simulations. For the present FCF calculation, we have restricted the vibrational transitions from $CH_2BrCl(\nu_1=0,\nu_2=0,\ldots,\nu_9=0)\rightarrow CH_2BrCl^+(\nu_1^+=x_1,\nu_2^+=x_2,\ldots,\nu_9^+=x_9)$, where each individual x_i could be any integer from 1 to 12 for $i=1-3$ and from 1 to 4 for $i=4-9$.

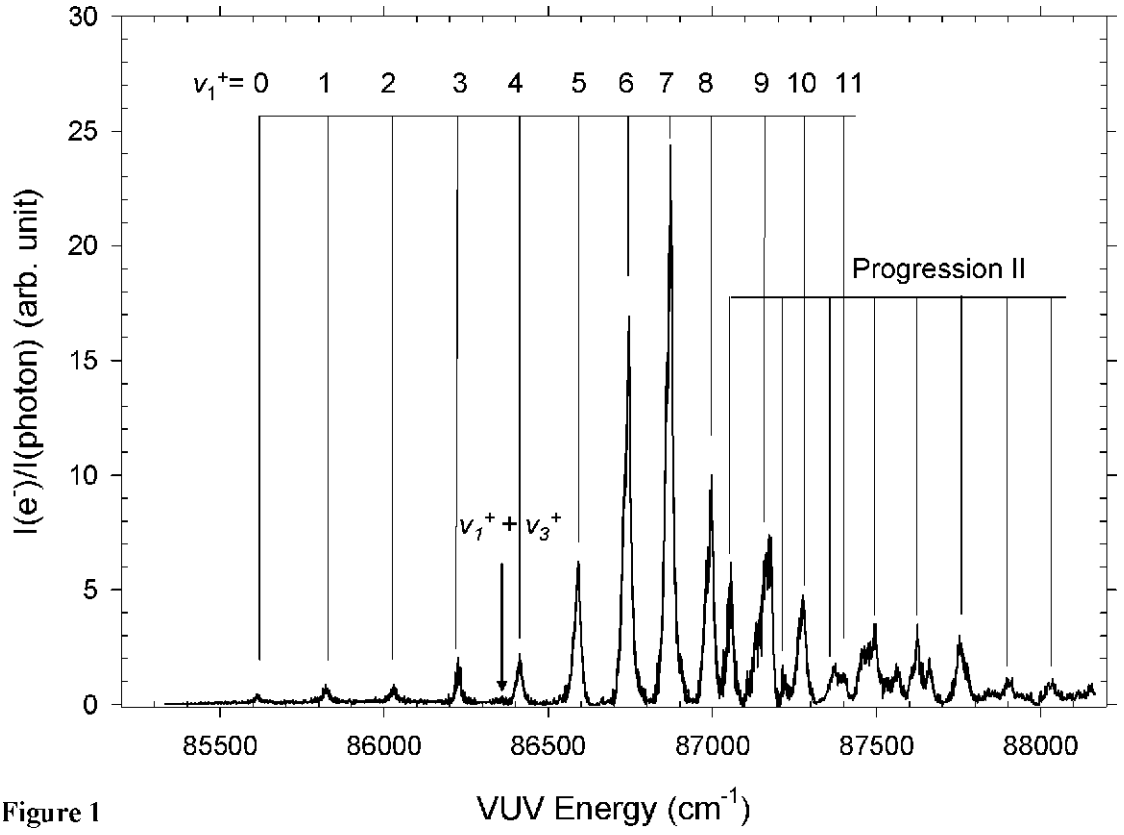

Figure 1

FIG. 1. The PFI-PE spectra of CH_2BrCl in the VUV energy range of 85 300–88 200 cm^{-1}. The $n\nu_1$ (n=0–11) progression are designated as progression I. The assignment of progression is tentative (see the text).

IV. RESULTS AND DISCUSSIONS

A. PFI-PE spectrum for $CH_2BrCl^+(\tilde{X}\,^2A')$

The VUV-PFI-PE spectrum of CH_2BrCl near its ionization onset in the VUV energy range of 85 330–88 160 cm^{-1} is shown in Fig. 1. We find that there are no PFI-PE structures at energies below 85 560 cm^{-1} and that the lowest vibrational band lies at 85 613.8 cm^{-1}. The spectrum of Fig. 1 reveals simple vibrational progression in the energy range from 85 618 to 86 998 cm^{-1}. At energies above 86 998 cm^{-1}, the PFI-PE spectrum shows more complex vibrational structures. Table III lists the peak positions and relative intensities of the prominent PFI-PE vibrational bands resolved in the spectrum of Fig. 1. We have arbitrarily normalized the intensity of the most intense PFI-PE vibrational band at 86 872.3 cm^{-1} to the value of 100.

There are nine vibrational modes for each of $CH_2BrCl(\tilde{X}\,^1A')$ and $CH_2BrCl^+(\tilde{X}\,^2A')$, of which six are of a' symmetry and three are of a'' symmetry. Although the experimental vibrational frequencies for the neutral $CH_2BrCl(\tilde{X}\,^1A')$ are known,[46,47] those for the cation $CH_2BrCl^+(\tilde{X}\,^2A')$ have not been measured experimentally. To assist the vibrational assignment of the PFI-PE spectrum, we have made a detailed comparison of the theoretical AH vibrational frequencies of $CH_2BrCl(\tilde{X}\,^1A')$ calculated at the MP2/6-311++G(2df,p), B3LYP/6-311++G(2df,p), and CCSD(T)/6-311++G(2df,p) levels with the experimental vibrational frequencies (see Table II). The deviations between the theoretical AH frequencies and the corresponding experimental frequencies are also given in parentheses in Table II. This comparison shows that the AH(MP2) and AH(B3) frequencies for $CH_2BrCl(\tilde{X}\,^1A')$ obtained by the CCSD(T)/6-311++G(2df,p) calculation are the most accurate, with the maximum discrepancy of $<2\%$. We note that the theoretical AH(MP2) and AH(B3) frequencies for the cation $CH_2BrCl^+(\tilde{X}\,^2A')$ are nearly identical except those for the ν_1^+ predictions, which differ by 11 cm^{-1}.

There are a total of 60 electrons in CH_2BrCl, populating 22 orbitals of a' symmetry and eight orbitals with a'' symmetry. The main electronic configuration for $CH_2BrCl(\tilde{X}\,^1A')$ is

$$\ldots\ldots (21a')^2(7a'')^2(22a')^2(8a'')^2, \quad \tilde{X}\,^1A'.$$

The orbitals $22a'$ and $8a''$ are the lone-pair orbitals associated with the Br atom in CH_2BrCl and differ by only $\approx$20 meV in energy. On the basis of the CCSD(T)/CBS calculation, the ground electronic state $CH_2BrCl^+(\tilde{X}\,^2A')$ is formed by the removal of an electron from the $22a'$ orbital. As shown in the comparison of the calculated bond distances (r) and bond angles ($\angle$) for $CH_2BrCl(\tilde{X}\,^1A')$ and $CH_2BrCl^+(\tilde{X}\,^2A')$ in Table I, the equilibrium $\angle$(Br–C–Cl) and r(C–Br) of the cation exhibit the largest changes from those of the neutral, indicating that the Cl–C–Br bending mode $\nu_1^+(a')$ and the C–Br stretching mode $\nu_2^+(a')$ of $CH_2BrCl^+(\tilde{X}\,^2A')$ are excited upon photoionization of

TABLE III. Vibrational progressions I and II observed in the VUV-PFI-PE spectrum for $CH_2BrCl^+(\tilde{X}\,^2A')$.

Band positions[a] (cm^{-1})				
Progression I	Progression II	Relative energies[b,c] (cm^{-1})	Normalized intensities[d,e]	Assignments
85 612.4		0.0	2(0.2)	0^{0+}
85 822.1		209.7(209.7)	4 (2)	$\nu_1^+=1$
86 028.9		416.5(206.8)	4 (8)	$\nu_1^+=2$
86 226.9		613.6(197.1)	9 (21)	$\nu_1^+=3$
86 413.1		799.8(186.2)	10 (42)	$\nu_1^+=4$
86 591.9		978.6(178.8)	26 (67)	$\nu_1^+=5$
86 746.3		1133.0(154.4)	70 (88)	$\nu_1^+=6$
86 872.3		1250.0(126.0)	100(100)	$\nu_1^+=7$
86 998.2		1384.9 (126)	44 (98)	$\nu_1^+=8$
	87 057	1445	27	
87 172		1563 (173)	32 (85)	$\nu_1^+=9$
	87 212	1599(155)	8	
87 279		1670 (107)	21 (66)	$\nu_1^+=10$
	87 370	1757(158)	9	
87 400		1791 (121)	7 (46)	$\nu_1^+=11$
	87 495	1882(125)	15	
	87 624	2011(129)	15	
	87 755	2140(131)	13	
	87 896	2281(141)	5	
	88 037	2422(141)	5	

[a]Band positions are peak positions of the vibrational bands, except that for $CH_2BrCl^+(\tilde{X}\,^2A';0^{0+})$.

[b]Energies measured with respect to the $CH_2BrCl^+(\tilde{X}\,^2A';0^{0+})$ origin band.

[c]The values in parentheses are vibrational spacings between adjacent vibrational bands.

[d]The normalized intensities are obtained by normalizing the most intense vibrational band ($\nu_1^+=7$) at 86 872.3 cm^{-1} to a value of 100.

[e]The values in parentheses are normalized FCFs, which are obtained by normalizing the highest FCF for the $\nu_1^+=7$ band to a value of 100.

$CH_2BrCl(\tilde{X}\,^1A')$. With the removal of an electron from the $22a'$ lone pair orbital of Br, some net bonding interaction between the Br and Cl atoms can occur, resulting in a significantly smaller $\angle$(Br–C–Cl) in CH_2BrCl^+ compared to that in $CH_2BrCl(\tilde{X}\,^1A')$. Due to the large change (21.5°) in $\angle$(Br–C–Cl) between the neutral and cation, we expect unfavorable FCFs for photoionization transitions near the IE(CH_2BrCl). This expectation is consistent with the observation of very low vibrational band intensities at the ionization onset and the increasing trend of the vibrational band intensities as energy is increased from the photoionization onset (see the PFI-PE spectrum of Fig. 1).

As expected, the FCF calculation based on the harmonic frequencies for the energy region of 0–2600 cm^{-1} above the IE(CH_2BrCl) predicts the dominant excitation of the $n\nu_1^+(a')$ ($n=0-12$) vibrational progression with the highest FCF predicted for the $7\nu_1^+(a')$ vibrational band of $CH_2BrCl^+(\tilde{X}\,^2A')$ formed in the photoionization of $CH_2BrCl(\tilde{X}\,^1A';0^0)$. Weaker vibrational progressions, $n\nu_1^+(a')+\nu_2^+(a')$ ($n=0-9$), $n\nu_1^+(a')+\nu_3^+(a')$ ($n=0-8$), and $n\nu_1^+(a')+\nu_6^+(a')$ ($n=0-6$), in the order of decreasing overall intensities are also predicted to be excited by the FCF calculation, where $\nu_2^+(a')$, $\nu_3^+(a')$, and $\nu_3^+(a')$ represents the respective C–Br stretching, C–Cl stretching, and CH_2 twisting modes of the cation. These combination bands have been observed previously in the PFI study of CH_2BrI by Lee *et al.*[48]

Guided by the FCF calculation, we have assigned the dominant PFI-PE bands to the $n\nu_1^+(a')$ ($n=0-11$) vibrational progression as marked in Fig. 1. The assignment and normalized FCFs (nFCFs) for the $n\nu_1^+(a')$ ($n=0-11$) vibrational progression, which is designated as progression I, are also given in Table II. For the sake of comparison with the relative vibrational band intensities, the nFCFs are obtained by arbitrarily scaling the FCF for the $7\nu_1^+(a')$ band to a value of 100. As shown in Table II, although quantitative agreement between the relative vibrational band intensities and nFCFs are not found, the trends of the normalized band intensities and nFCFs are in good accord with the $7\nu_1^+(a')$ band exhibiting the highest intensity or nFCF. The spacings of adjacent vibrational bands for the $n\nu_1^+(a')$ ($n=0-11$) progression are also included in Table II. The first vibrational spacing between $\nu_1^+(a')=0$ and 1 is 209.7 ± 2.0 cm^{-1} and is in excellent agreement with the AH $\nu_1^+(a')$ vibrational frequency prediction (212 cm^{-1}) calculated at the B3LYP/6-311++G(2df,p) level and the AH(MP2) $\nu_1^+(a')$ vibrational frequency prediction of 216 cm^{-1} calculated at the CCSD(T)/6-311++G(2df,p) level of theory. This, together with the fact that the experimental $\nu_1^+(a')$ frequency is lower than the $\nu_1(a')$ frequency, indicates that the AH(MP2) vibrational frequency predictions are more accurate than the AH(B3) values for CH_2BrCl and CH_2BrCl^+. The predicted AH vibrational frequency for $\nu_1^+(a')$ at the MP2/6-311+

+G(2df,p) level differs a lot from the B3LYP and CCSD(T) predictions. This assignment identifies the vibrational band at 85 614 cm^{-1} as the origin or 0^{0+} band of $CH_2BrCl^+(\tilde{X})$. No hot bands were observed below this band. In order to obtain a more precise value for the adiabatic IE of CH_2BrCl, we have performed a semiempirical simulation of the origin band using a method described previously. The simulation used the theoretical rotational constants for CH_2BrCl (A =0.9836 cm^{-1}, B=0.068 26 cm^{-1}, C=0.064 63 cm^{-1}) and CH_2BrCl^+ (A^+=0.6963 cm^{-1}, B^+=0.087 41 cm^{-1}, C^+ =0.078 91 cm^{-1}) and assumed a rotational temperature of 12 K. On the basis of the semiempirical simulation, the adiabatic IE(CH_2BrCl) is determined to 85 612.4±2.0 cm^{-1} (10.6146±0.0003 eV), which is found to be lower than the previous He I and PIE determination[18,19] (10.77 eV) by 0.16 eV.

The $n\nu_1^+(a')$ (n=0–6) vibrational band positions and their adjacent vibrational spacings, i.e., 209.7, 206.8, 197.1, 186.2, 178.8, and 154.4 cm^{-1}, appear to be consistent with those expected based on the anharmonic oscillator vibrational term, $G(\nu)=\tilde{\nu}_1^+(\nu^+ +1/2)-\tilde{\nu}_1^+\chi_1^+(\nu^+ +1/2)^2$. By fitting the observed vibrational level positions for $n\nu_1^+(a')$ (n =0–6) to the latter equation, we obtain $\tilde{\nu}_1^+$=225.0 cm^{-1} and $\tilde{\nu}_1^+\chi_1^+$=5.2 cm^{-1}. The adjacent vibrational spacings (126.0, 126, 173, 107, and 121) obtained for the $n\nu_1^+(a')$ (n =6–11) bands based on the present assignment are irregular, indicating the occurrence of strong perturbations. Thus, these members of progression I may not be pure $\nu_1^+(a')$ vibrational bands. This interpretation is consistent with the observation that the PFI-PE features resolved in Fig. 1 at energies above the $7\nu_1^+(a')$ band position (86 872.3 cm^{-1}) are more complex, consisting of overlapping vibrational structures. We have grouped the majority of these structures into progression II. The fact that the average vibrational spacing for progression II is 140 cm^{-1} suggests that this progression may consist mainly of higher members of the combination bands, such as $\nu_2^+(a')+n\nu_1^+(a')$, or/and $\nu_3^+(a')+n\nu_1^+(a')$, which are predicted by the FCF calculation. The present assignment of progression II and the higher members n=9–11 of progression I must be viewed as tentative. A higher resolution study is needed in the future to identify the combination bands $n\nu_1^+(a')+\nu_2^+(a')$, $n\nu_1^+(a')+\nu_3^+(a')$, and $n\nu_1^+(a')+\nu_6^+(a')$, which are predicted by the FCF calculation.

A careful examination of the spectrum reveals a very weak vibrational band at 744 cm^{-1} (marked by arrow in Fig. 1) above the origin band. Based on the theoretical vibrational frequency and FCF calculations, we have assigned this weak band as the $\nu_1^+(a')+\nu_2^+(a')$ combination band for the cation. Considering that the experimental $\nu_1^+(a')$=210 cm^{-1}, we obtained an estimate of 534 cm^{-1} for the $\nu_2^+(a')$.

As pointed out above, the two highest occupied orbitals, $22a'$ and $8a''$, only differ by ≈20 meV. At the CCSD(T)/CBS level, the ejection of an electron from the $22a'$ and $8a''$ lone pair orbitals produced the $CH_2BrCl^+(\tilde{X}\,^2A')$ and $CH_2BrCl^+(\tilde{A}\,^2A'')$ ion states, respectively. The excited $CH_2BrCl^+(\tilde{A}\,^2A'')$ state is predicted to lie at an energy of 0.174 eV or 1403 cm^{-1} above that of the $CH_2BrCl^+(\tilde{X}\,^2A')$ ground state. Thus, the perturbation observed for PFI-PE bands at energies above the $7\nu_2^+(a')$ level can be attributed to perturbation by the low lying excited $CH_2BrCl^+(\tilde{A}\,^2A'')$ state.

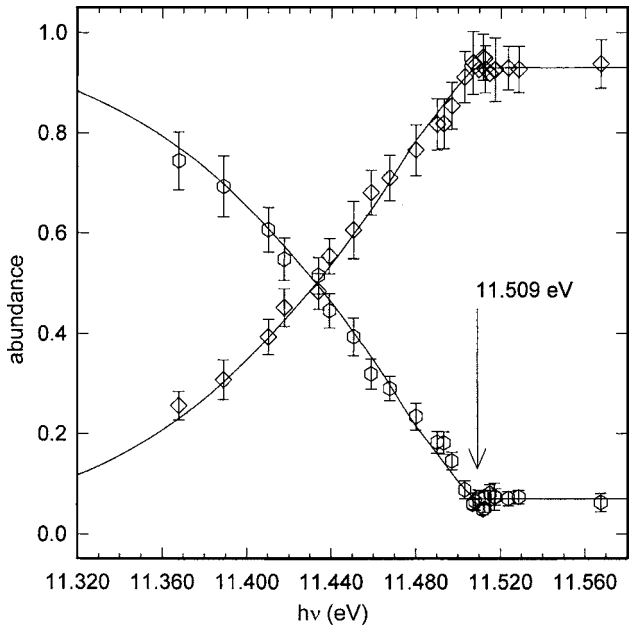

FIG. 2. The breakdown curves for parent CH_2BrCl^+ (open diamonds) and daughter CH_2Cl^+ (open circles) in the photon energy ($h\nu$) range of 11.320–11.580 eV obtained from PFI-PEPICO TOF measurements. The 0 K AE is determined by the break (marked by arrow) for the parent ion. The solid lines are the simulation curves. Error bars given in the figures reflect the counting statistics.

B. Energy-selected dissociation of CH_2BrCl^+ to form $CH_2Cl^+ + Br$

Figure 2 depicts the breakdown curves for parent CH_2BrCl^+ and daughter CH_2Cl^+ derived from the PFI-PEPICO TOF measurements in the VUV energy range of 11.364–11.564 eV. The procedures used in constructing the breakdown curves for the parent and daughter ions based on PFI-PEPICO TOF measurements have been described previously.[9–16] The breakdown diagram basically consists of the fractional abundances for the parent CH_2BrCl^+ ion (empty circles) and the daughter CH_2Cl^+ ion (empty diamonds) plotted as a function of photon energy in eV. Error bars calculated for individual data points as shown in Fig. 2 reflect the counting statistics. The fractional abundances of CH_2BrCl^+ and CH_2Cl^+ are defined as $I(CH_2BrCl^+)/[I(CH_2BrCl^+)+I(CH_2Cl^+)]$ and $I(CH_2Cl^+)/[I(CH_2BrCl^+)+I(CH_2Cl^+)]$, respectively. Here $I(CH_2BrCl^+)$ and $I(CH_2Cl^+)$ represent the relative intensities for CH_2BrCl^+ and CH_2Cl^+, which were measured by their respective TOF peak areas observed in the PFI-PEPICO TOF spectra.

The breakdown diagram of Fig. 2 has been simulated using a procedure described previously.[49] In the ideal situation with a 0 K gas sample, the breakdown curve for the parent (daughter) ion should switch from a fractional abundance of one to zero (zero to one) at the 0 K AE. In a realistic experiment with the gas sample at a finite temperature T, the available thermal rotational and vibrational excitations also contribute to the dissociation. This leads to the smoothing of the breakdown curves. As shown in previous PFI-

TABLE IV. The individual energetic contributions to the CCSD(T, full)/CBS predictions of the IE(CH_2ClBr), IE(CH_2Cl), and AE(CH_2Cl). Energy differences (ΔE's), IE, and AE are in eV.

		IE(CH_2ClBr)	IE(CH_2Cl)	AE(CH_2Cl^+)
$\Delta E_{extrapolated}$[a]	CBS_{TQ5}	10.661	8.683	11.740
	CBS_{Q5}	10.672	8.690	11.753
	Average	10.667	8.687	11.747
ΔZ_{ZPVE}[b]	MP2	−0.012	0.078	−0.099
	B3LYP	−0.012	0.074	−0.099
	Average	−0.012	0.076	−0.099
ΔE_{CV}[c]		0.027	0.012	0.035
ΔE_{SR}[d]		−0.034	−0.008	−0.023
ΔE_{SO}[e]		−0.027	···	−0.152
CCSD(T, full)/CBS IE or AE[f]		10.621	8.767	11.508
Experiment		10.6146[g] ±0.0003 eV	8.75±0.01[h]	11.509[g] ±0.002

[a]Extrapolated from the frozen-core total energies using Eqs. (1) and (2).
[b]Taken as the sum of all anharmonic vibrational frequencies at CCSD(T)/6-311++G(2df,p). Both anharmonic vibrational frequencies with anharmonicity corrections done at MP2 and B3LYP levels are included.
[c]Core-valence electrons correlation obtained as the difference of all-electron and frozen-core energies at CCSD(T) using aug-cc-pwCVQZ basis set.
[d]Scalar relativistic effect calculated at CISD/aug-cc-pV5Z.
[e]Atomic spin-orbit coupling for chlorine is taken from Ref. 40. See the text for the molecular spin-orbit coupling calculations of CH_2BrCl^+.
[f]CCSD(T,full)/CBS AE or IE=$\Delta E_{extrapolated\ CBS}+\Delta E_{ZPCV}+\Delta E_{CV}+\Delta E_{SR}+\Delta E_{SO}$.
[g]This work.
[h]Reference 52.

PEPICO studies, the temperature T used here in the simulation of the breakdown curves need not be the actual beam temperature of the gas sample because PFI depends on the Stark field effect and the lifetime switching effect[50] at energies near the dissociation threshold. These effects lead to a more complex mechanism than can be accounted for by a simple statistical theory. Based on the known vibrational frequencies and calculated rotational constants for CH_2BrCl, we calculated the density of rovibrational states using the Beyer-Swinehart direct count algorithm.[51] No efforts were made to analyze the cold components of the parent and daughter ion signal. The overall fits to the breakdown data by assuming T=280 K for the parent molecules are shown as solid lines in Fig. 2. The simulation also takes into account the uniform coincidence background of 6%, which results from the dispersion of prompt electrons into the dark gap of the synchrotron period. The simulation yields a value of 11.509 eV for the 0 K AE(CH_2Cl^+).

We have demonstrated previously in PFI-PEPICO TOF experiments that the disappearance energy for the parent ion is an intrinsic feature for identifying the 0 K AE of the dissociation process.[7–16] If the coincidence measurement has a constant coincidence background as is observed in the present case, the breakdown curve should exhibit a break at the 0 K AE (see the break marked by arrow in Fig. 2). The 0 K AE(CH_2Cl^+)=11.509±0.002 eV determined based on this break is unambiguous and does not depend on the statistical simulation. Nevertheless, the agreement observed between the 0 K AE(CH_2Cl^+) value obtained by the break and that by the statistical simulation gives a physical interpretation for the observed break in the breakdown diagram. The assigned error limit of ±0.002 eV has taken into account the uncertainty due to the VUV energy calibration.

Combining the AE(CH_2Cl^+) derived by the PFI-PEPICO study and the IE(CH_2BrCl) value determined by the PFI-PE measurement, we obtain the D_0(CH_2Cl^+−Br) =0.894±0.002 eV. The IE(CH_2Cl^+)=8.75±0.01 eV has been determined in a previous He I study.[52] This value, together with the AE(CH_2Cl^+) obtained here, allows the determination of the D_0(CH_2Cl−Br)=2.76±0.01 eV.

C. CCSD(T)/CBS predictions for IE(CH_2BrCl), IE(CH_2Cl), and AE(CH_2Cl^+)

The CCSD(T)/CBS predictions for the IE(CH_2BrCl), IE(CH_2Cl), and AE(CH_2Cl^+), together with individual energetic contributions ($\Delta E_{extropolatedCBS}$, ΔE_{ZPVE}, ΔE_{CV}, ΔE_{SR}, and ΔE_{SO}) to these predictions are listed in Table IV. The experimental IE(CH_2BrCl), IE(CH_2Cl),[51] and AE(CH_2Cl^+) are also given in Table IV for comparison with the theoretical predictions. After taking into account of the high-level corrections ($\Delta E_{ZPVE}+\Delta E_{CV}+\Delta E_{SR}+\Delta E_{SO}$), the CCSD(T, full)/CBS calculations yield the predictions IE(CH_2BrCl) =10.621 eV, IE(CH_2Cl)=8.767 eV, and AE(CH_2Cl^+) =11.508 eV. These values allow the calculation of the CCSD(T)/CBS predictions for D_0(CH_2Cl^+−Br)=0.887 eV and D_0(CH_2Cl−Br)=2.741 eV. As shown in Table IV, the $\Delta E_{extropolatedCBS}$ values for the IE(CH_2BrCl) and AE(CH_2Cl^+) obtained by the two extrapolation schemes differ by 11 and 13 meV, respectively. The differences in $\Delta E_{extropolatedCBS}$ based on the two extrapolation schemes for the IE(CH_2Cl) are found to be 7 meV. The differences ($\leqslant$4 meV) of the ΔE_{ZPVE} values based on the AH(MP2) and AH(B3) frequencies for the IE and AE calculations appear to be small. These differences set the minimum error limit of the CCSD(T)/CBS predictions.

The CCSD(T)/CBS predictions for the IE(CH_2BrCl), AE(CH_2Cl^+), and $D_0(CH_2Cl^+-Br)=0.894\pm0.002$ eV are in excellent accord with the experimental IE(CH_2BrCl) $=10.6148\pm0.0003$ eV and AE(CH_2Cl^+)$=11.509\pm0.002$ eV determined in the present study. The CCSD(T)/CBS IE(CH2Cl) value is also in agreement with the He I experimental IE(CH_2Cl)$=8.75\pm0.01$ eV.[52]

V. CONCLUSIONS

The spectroscopy of $CH_2BrCl^+(\tilde{X})$ and the D_0 values for CH_2Cl-Br and CH_2Cl^+-Br have been investigated using VUV laser and synchrotron based PFI methods, together with *ab initio* calculations performed at the CCSD(T, full)/CBS level with high-level corrections. Both the experiment and theoretical calculations of this study show that the bending modes for $CH_2BrCl^+(\tilde{X})$ are strongly excited upon photoionization of $CH_2BrCl(\tilde{X})$. The assignment of the PFI-PE spectrum for CH_2BrCl gives the Br–C–Cl bending vibrational frequency $\nu_1^+=209.7\pm2.0$ cm^{-1} for $CH_2BrCl^+(\tilde{X})$ and the adiabatic IE(CH_2BrCl)$=85\,612.4\pm2.0$ cm^{-1} (10.6146 ± 0.0003 eV). The present theoretical study also accounts for the perturbed structures observed in the PFI-PE spectrum at energies ≈1300 cm^{-1} above the IE(CH_2BrCl). Furthermore, we have determined a highly precise value of 11.509 ± 0.002 eV for the 0 K AE(CH_2Cl^+) by PFI-PEPICO TOF measurements. These IE(CH_2BrCl) and 0 K AE(CH_2Cl^+) values, together with the known IE(CH_2Cl), have allowed the determination of the $D_0(CH_2Cl^+-Br)=0.894\pm0.002$ eV and $D_0(CH_2Cl-Br)=2.76\pm0.01$ eV. Comparing these experimental IE(CH_2BrCl), IE(CH_2Cl), AE(CH_2Cl^+), $D_0(CH_2Cl^+-Br)$, and $D_0(CH_2Cl-Br)$ with CCSD(T)/CBS predictions, we conclude that the CCSD(T)/CBS procedures with high level corrections are highly accurate with an estimated error of <17 meV.

ACKNOWLEDGMENTS

One of the authors (Y.M.) acknowledges the support by the National Science Foundation of China Project No. 20673066 and by the Chinese Ministry of Education of China Project No. 10274041. One of the authors (K.C.L.) acknowledges the support from the Department of Biology and Chemistry at the City University of Hong Kong. One of the authors (C.Y.N.) acknowledges the support by the U.S. Department of Energy, Office of Basic Energy Sciences, Division of Chemical Sciences, Geosciences, and Biosciences under Contract No. DE-FG02-02ER15306. The calculations of this work were performed using the Molecular Science Computing Facility (MSCF) in the William R. Wiley Environmental Molecular Sciences Laboratory, a national scientific user facility sponsored by the U.S. Department of Energy's Office of Biological and Environmental Research. Part of the calculations of this work used resources of the National Energy Research Scientific Computing Center, which is supported by the Office of Science of the U.S. Department of Energy under Contract No. DE-AC03-76SF00098. One of the authors (C.Y.N.) also acknowledges partial supports by the AFOSR Grant No. FA9550-06-1-0073, and the NSF Grant No. CHE-0517871. One of the authors (K.C.L.) acknowledges Professor K. A. Peterson for providing the aug-cc-pwCVQZ basis sets of Br prior to publications.

[1] M. J. Molina, L. T. Molina, and C. E. Kolb, Annu. Rev. Phys. Chem. **47**, 327 (1996).
[2] C. W. Spicer, E. G. Chapman, B. J. Finlayson-Pitts, R. A. Plastridge, J. M. Hubbe, J. D. Fast, and C. M. Berkowitz, Nature (London) **394**, 353 (1998).
[3] F. S. Rowland, Annu. Rev. Phys. Chem. **42**, 731 (1991).
[4] L. A. Barrie, J. W. Bottenheim, R. C. Schnell, P. J. Crutzen, and R. A. Rasmussen, Nature (London) **334**, 138 (1988).
[5] T. Zhang, C. Y. Ng, C.-S. Lam, and W.-K. Li, J. Chem. Phys. **123**, 174316 (2005).
[6] J. Zhou, K.-C. Lau, E. Hassanein, H. Xu, S.-X. Tian, B. Jones, and C. Y. Ng, J. Chem. Phys. **124**, 034309 (2006).
[7] C. Y. Ng, Annu. Rev. Phys. Chem. **53**, 101 (2002).
[8] G. K. Jarvis, K.-M. Weitzel, M. Malow, T. Baer, Y. Song, and C. Y. Ng, Rev. Sci. Instrum. **70**, 3892 (1999).
[9] K.-M. Weitzel, M. Malow, G. K. Jarvis, T. Baer, Y. Song, and C. Y. Ng, J. Chem. Phys. **111**, 8267 (1999).
[10] G. K. Jarvis, K.-M. Weitzel, M. Malow, T. Baer, Y. Song, and C. Y. Ng, Phys. Chem. Chem. Phys. **1**, 5259 (1999).
[11] Y. Song, X.-M. Qian, K.-C. Lau, C. Y. Ng, J. Liu, and W. Chen, J. Chem. Phys. **115**, 2582 (2001).
[12] Y. Song, X.-M. Qian, K.-C. Lau, C. Y. Ng, J. Liu, and W. Chen, J. Chem. Phys. **115**, 4095 (2001).
[13] X.-M. Qian, Y. Song, K.-C. Lau, C. Y. Ng, J. Liu, and W. Chen, Chem. Phys. Lett. **347**, 51 (2001).
[14] X.-M. Qian, Y. Song, K.-C. Lau, C. Y. Ng, J. Liu, W. Chen, and G.-Z. He, Chem. Phys. Lett. **353**, 19 (2002).
[15] X.-M. Qian, K.-C. Lau, and C. Y. Ng, J. Chem. Phys. **120**, 11031 (2004).
[16] X. N. Tang, Y. Hou, C. Y. Ng, and B. Ruscic, J. Chem. Phys. **123**, 074330 (2005).
[17] K.-C. Lau and C.-Y. Ng, Acc. Chem. Res. **39**, 823 (2006).
[18] K. Watanabe, T. Nakayama, and J. Mottl, J. Quant. Spectrosc. Radiat. Transf. **2**, 369 (1962).
[19] I. Novak, T. Cvitas, L. Klasinc, and H. Gusten, J. Chem. Soc., Faraday Trans. 2 **77**, 2049 (1981).
[20] A. G. Harrison and T. W. Shannon, Can. J. Chem. **40**, 1730 (1962).
[21] X. M. Qian, Y. Song, C. Y. Ng, W. Chen, and J. Liu, *Abstract of Papers of the American Chemical Society* 221:40-PHYS, Part 2, April 1, 2001.
[22] A. F. Lago, J. P. Kercher, A. Bodi, B. Sztaray, B. Miller, D. Wurzelmann, and T. Baer, J. Phys. Chem. A **109**, 1802 (2005).
[23] K. C. Lau and C. Y. Ng, J. Chem. Phys. **122**, 224310 (2005).
[24] K.-C. Lau and C. Y. Ng, J. Chem. Phys. **124**, 044323 (2006).
[25] K.-C. Lau and C. Y. Ng, Chin. J. Chem. Phys. **19**, 29 (2006).
[26] Y. Mo, J. Yang, and C. Chen, J. Chem. Phys. **120**, 1263 (2004).
[27] J. Yang, Y. Mo, K. C. Lau, Y. Song, X. M. Qian, and C. Y. Ng, Phys. Chem. Chem. Phys. **7**, 1518 (2005).
[28] P. Heimann, M. Koike, C.-W. Hsu *et al.*, Rev. Sci. Instrum. **68**, 1945 (1997).
[29] C.-W. Hsu, M. Evans, P. A. Heimann, and C. Y. Ng, Rev. Sci. Instrum. **68**, 1694 (1997).
[30] G. K. Jarvis, Y. Song, and C. Y. Ng, Rev. Sci. Instrum. **70**, 2615 (1999).
[31] S. Stimson, Y.-J. Chen, M. Evans, C.-L. Liao, C. Y. Ng, C.-W. Hsu, and P. Heimann, Chem. Phys. Lett. **289**, 507 (1998).
[32] K. Raghavachari, G. W. Trucks, J. A. Pople, and M. Head-Gordon, Chem. Phys. Lett. **157**, 479 (1989).
[33] D. A. Dixon, D. Feller, and K. A. Peterson, J. Chem. Phys. **115**, 2576 (2001), and references therein.
[34] T. H. Dunning Jr., J. Chem. Phys. **90**, 1007 (1989); R. A. Kendall, T. H. Dunning Jr., and R. J. Harrison, *ibid.* **96**, 6796 (1992); T. H. Dunning Jr., K. A. Peterson, and A. K. Wilson, *ibid.* **114**, 9244 (2001); A. K. Wilson, D. E. Woon, K. A. Peterson, and T. H. Dunning, *ibid.* **110**, 7667 (1999).
[35] K. A. Peterson, D. E. Woon, and T. H. Dunning Jr., J. Chem. Phys. **100**, 7410 (1994).
[36] T. Helgaker, W. Klopper, H. Koch, and J. Nago, J. Chem. Phys. **106**, 9639 (1996); A. Halkier, T. Helgaker, P. Jorgensen, W. Klopper, H. Koch, J. Olsen, and A. K. Wilson, Chem. Phys. Lett. **286**, 243 (1998).
[37] R. S. Grev, C. L. Janssen, and H. F. Schaefer, J. Chem. Phys. **95**, 5128 (1991); V. Barone, *ibid.* **120**, 3059 (2004).
[38] K. A. Peterson and T. H. Dunning Jr., J. Chem. Phys. **117**, 10548 (2002).

[39] E. R. Davidson, Y. Ishikawa, and G. L. Malli, Chem. Phys. Lett. **84**, 226 (1981).
[40] C. E. Moore, *Atomic Energy Levels*, Natl. Bur. Stand. (U.S.) Circ. No. 467 (U.S. GPO, Washingtons, D.C., 1949).
[41] A. Berning, M. Schweizer, H.-J. Werner, P. J. Knowles, and P. Palmieri, Mol. Phys. **98**, 1823 (2000).
[42] H.-J. Werner, P. J. Knowles, R. D. Amos *et al.*, computed code MOLPRO, University College of Cardiff Consultants Limited, Cardiff, UK, 2006.
[43] M. J. Frisch, G. W. Trucks, H. B. Schlegel *et al.*, GAUSSIAN 03, Revision B.05, Gaussian, Inc., Pittsburgh, Pennsylvania, 2003.
[44] MOMOFCF program can be obtained from http://hera.ims.ac.jp
[45] M. Yamaguchi, T. Momose, and T. Shida, J. Chem. Phys. **93**, 4211 (1990).
[46] S. Giorgianni, B. De Carli, R. Visinoni, and S. Ghersetti, Spectrosc. Lett. **19**, 1207 (1986).
[47] A. Weber, A. G. Meister, and F. F. Cleveland, J. Chem. Phys. **21**, 930 (1953).
[48] M. Lee, H. Kim, Y. S. Lee, and M. S. Kim, J. Chem. Phys. **123**, 024310 (2005).
[49] T. Baer, Y. Song, C. Y. Ng, J. Liu, and W. Chen, Faraday Discuss. **115**, 137 (2000).
[50] K.-M. Weitzel, G. Jarvis, M. Malow, T. Baer, Y. Song, and C. Y. Ng, Phys. Rev. Lett. **86**, 3526 (2001).
[51] Y. Song, X.-M. Qian, K.-C. Lau, C. Y. Ng, J. Liu and W. Chen, J. Chem. Phys. **115**, 4095 (2001).
[52] L. Andrews, J. M. Dyke, N. Jonathan, N. Keddar, and A. Morris, J. Am. Chem. Soc. **106**, 229 (1984).